The role of anlotinib-mediated EGFR blockade in a positive feedback loop of CXCL11-EGF-EGFR signalling in anaplastic thyroid cancer angiogenesis

Supplementary Table legends

Table S1. Sense and anti-sense sequences of siRNA used in this study.

Table S2. Primers used in this study.

Table S3. IC50 values of anlotinib in ATC cell lines. IC50 50% inhibitory concentration.

Supplementary Figure legends

Figure S1. Anlotinib suppresses hypoxia-activated angiogenesis in ATC. **A.** ATC cells were treated with control medium or a series of concentration of anlotinib (0.5, 1, 2, 5, 10, 20, 40 and 80 μM) under hypoxia for 24 h, 48 h and 72 h. Cell viability was assessed by CCK-8 assay (hypoxia: 2% concentration of O_2). **B-C.** HUVEC was incubated with supernatants from CAL-62 and KHM-5M cells treated with hypoxia or anlotinib. Angiogenic assays included tubule formation, HUVEC migration, 3D sprouting and CAM assay. Data were obtained from three independent experiments. **D.** EndMT markers (αSMA, Vimentin and Snail) were detected in HUVEC incubated with supernatants from CAL-62 and KHM-5M cells treated with hypoxia or anlotinib. Representative WB and its quantification from three independent experiments were shown. **E.** Immunofluorescence of αSMA and Vimentin were detected in HUVEC incubated with supernatants from CAL-62 and KHM-5M cells treated with hypoxia or anlotinib. Representative images and its quantification from three independent

experiments were shown. *$p < 0.05$; **$p < 0.01$.

Figure S2. CXCL11 mediates anlotinib inhibition of hypoxia-activated angiogenesis. **A.** Angiogenesis antibody array was performed. CAL-62 was pre-incubated under hypoxia for 24 h. Control medium and anlotinib (5 μM) were added into CAL-62 for another 24 h under hypoxia (2% concentration of O_2). Left images are the raw experimental array, and the gray density represents the protein expressive level in each group (Control vs Anlotinib). There are two panels with different targets for each group. In each panel, every dot symbolizes an antibody target, and every target is spotted in duplicate vertically. Right tables are the corresponding molecular name of raw data in left panels. The most significant change protein expression is framed using Red or Green. Red means the increased expressions after Anlotinib exposure, whereas, Green means the decreased expressions. **B.** Venn diagram of anlotinib-downregulated factors and HIF1α-induced angiogenic genes. CXCL11, MMP9, VEGFR2 and GCSF were downregulated by anlotinib and also induced by HIF1α. **C.** The production of MMP9, GCSF and VEGFR2 was assayed under hypoxia or anlotinib treatment. **D**&**E**. Elisa (**D**) and PCR (**E**) targeting CXCL11 confirmed that anlotinib could decrease the hypoxia-upregulated of CXCL11 expression. **F-G.** Adding rhCXCL11 into the supernatants collected from CAL-62 and KHM-5M cells treated with anlotinib could reverse anlotinib's anti-angiogenic abilities; adding CXCL11 neutralize antibody into the supernatants collected from CAL-62 and KHM-5M cells treated with hypoxia

could partly attenuate hypoxia-induced angiogenesis. **H.** EndMT markers (αSMA and Vimentin) stressed the necessity of CXCL11 in promoting or inhibiting EndMT by hypoxia or anlotinib, respectively. All data were obtained from three independent experiments. *$p < 0.05$; **$p < 0.01$.

Figure S3. CXCL11 promotes angiogenesis by promoting EGF expression in ATC. **A.** The representative IHC images of positive and negative CXCL11 in tumour and peritumour, respectively. Tissue microarray included a cohort of ATC tumour with matched peritumuor tissues from 25 patients. Twenty-five patients (16 females and 9 males) had a mean age of 59.96 ± 13.50 years. All patients were categorized as stage IV according to AJCC TNM staging system. The average survival time was 2.56 ± 1.34 months. **B.** CXCL11 expression in multiple ATC cell lines was examined. **C.** rhCXCL11 (100 ng/mL for 2 h) was proved to promote tube formation and migration in HUVEC. **D.** CXCL11 was ectopically overexpressed and knocked down in CAL-62 and KHM-5M cells. **E-G.** Supernatants from CAL-62 and KHM-5M cells with CXCL11 silencing leaded to repressed tube formation and migration (**E**), EndMT (**F**) and HUVEC proliferation (**G**). **H-J.** Supernatants from CAL-62 and KHM-5M with CXCL11 overexpression could improve tube formation and migration abilities (**H**) and EndMT (**I**), and HUVEC proliferation (**J**). **K.** PCRs of EGF, CXCL5, LEP, TPO and IGNG were completed in HUVEC exposed with rhCXCL11 (100 ng/ml for 2 h) against negative control. **L.** CXCR7 and CXCR3 were knocked down by siRNA in HUVEC. **M.** mRNA production of EGF increased under rhCXCL11 treatment (100

ng/ml for 2 h), when silencing CXCR3 but not CXCR7. **N.** mRNA production of CXCL11 was not significantly changed after rhCXCL11 incubation. The high amount CXCL11 protein in Western Blot, independent to CXCR3 or CXCR7 knockdown, was mainly from exogenously administrated rhCxcl11, but not produced by cells themselves. **O.** The apoptotic rate of HUVEC/siNC and HUVEC/siCXCR7 incubated with rhCXCL11. **P.** CXCR7 production in HUVEC incubated with rhCXCL11; CXCR7 production in HUVEC/siEGFR against HUVEC/siNC. **Q**. Basal expression of CXCR7 in ATC cells and HUVEC. **R.** The expression levels of p-EGFR, αSMA and Vimentin in HUVEC/siNC and HUVEC/siEGFR incubated with rhEGF (10 nmol/L for 5 minutes). All data are obtained from three independent experiments. *$p < 0.05$; **$p < 0.01$. (AJCC: American Joint Committee on Cancer; Demographic data was presented as mean ± SD).

Figure S4. EGFR upregulates CXCL11 in a positive feedback loop in ATC. **A.** The representative IHC images of positive and negative phospho-EGFR (phospho-Y1068) in tumour and peritumour, respectively. **B.** Expression of phospho-EGFR in multiple ATC cell lines. **C&D.** CXCL11 production and AKT-mTOR signaling were increased in CAL-62 and KHM-5M cells with EGFR overexpression (**C**) and rhEGF incubation (**D**). **E.** Adding rhCXCL11 into the supernatants from CAL-62 and KHM-5M with EGFR knockdown could partly relieved the reduced tubule formation and cell migration. **F.** EndMT markers were examined when rhCXCL11 added into the supernatants from CAL-62 and KHM-5M

cells with EGFR knockdown. **G.** Adding anti-CXCL11 into the supernatants from CAL-62 and KHM-5M with EGFR overexpression could attenuate the EGFR-promoted tubule formation and migration. **H.** EndMT markers were examined when anti-CXCL11 added into the supernatants of CAL-62 and KHM-5M cells with EGFR overexpression. All data were obtained from three independent experiments. *$p < 0.05$; **$p < 0.01$.

Figure S5. Anlotinib directly targets EGFR kinase. **A.** Phospho-RTK antibody array was performed in CAL-62. This array was completed with the same samples as that in angiogenesis antibody array. Left images are the raw experimental array, and the gray density represents the protein expressive level in each group (Control vs Anlotinib). Every dot symbolizes an antibody target, and every target is spotted in duplicate horizontally. Right tables are the corresponding molecular name of raw data in left images. The most significant change protein expression is framed using Red or Green. Red means the increased expressions after Anlotinib exposure, whereas, Green means the decreased expressions. **B.** Representative WBs of p-EGFR, p-FGFR1, p-ALK and p-JAK2 expressions in CAL-62, KHM-5M, BHT101 and C643 treated by anlotinib or control medium. **C.** Cartoon representations of anlotinib occupying the binding pocket of EGFR. **D.** Anlotinib repressed angiogenetic abilities by directly inhibiting HUVEC, including tubule formation, migration, 3D sprouting buddings and CAM vessels. All data were obtained from three independent experiments.

Table S1. Sense and anti-sense sequences of siRNA used in this study.

Genes	siRNA	Sense	Anti-sense
EGFR	si1	CCUCCAGAGGAUGUUCAAUAATT	UUAUUGAACAUCCUCUGGAGGTT
	si2	GCCAAGCCAAAUGGCAUCUUUTT	AAAGAUGCCAUUUGGCUUGGCTT
	si3	GCCACAAAGCAGUGAAUUUAUTT	AUAAAUUCACUGCUUUGUGGCTT
CXCL11	si1	CCUUCUAGAUUUGAUGCUUTT	AAGCAUCAAAUCUAGAAGGTT
	si2	GGGAGACAUUCUUAUGCAUTT	AUGCAUAAGAAUGUCUCCCTT
	si3	GGUAUACUCAAGACUAGUUTT	AACUAGUCUUGAGUAUACCTT
CXCR3	si1	UUUAGUCUGUGAUUUACUCUG	GAGUAAAUCACAGACUAAAUC
	si2	ACUCUUUUGUGAUUGAGUCUG	GACUCAAUCACAAAAGAGUUC
	si3	AGAAGUUGAUGUUGAAGAGGG	CUCUUCAACAUCAACUUCUAC
CXCR7	si1	UUGUACUAGGCAAAACCAGCC	CUGGUUUUGCCUAGUACAAGG
	si2	UAACAAUCCUUGUACUAGGCA	CCUAGUACAAGGAUUGUUACC
	si3	UAGAAAAAAGCAUAUGCACCC	GUGCAUAUGCUUUUUUCUAGG

Table S2. Primers used in this study.

Gene	Sense primer 5′-3′	Anti-sense primer 5′-3′
CXCL5	TGTTGGTGCTGCTGCTGCTG	GGATGAACTCCTTGCGTGGTCTG
LEP	ATTTCACACACGCAGTCAGTCTCC	CCCAGGCTGTCCAAGGTCTCC
TPO	GCTGTCTGTCACGCTGGTTATGG	AATCACTCCGCTTGTTGGCTCAG
IFNG	TTGGGTTCTCTTGGCTGTTACTGC	TGCTTTGCGTTGGACATTCAAGTC
CXCL11	TGCTACAGTTGTTCAAGGCTTCCC	CTGCCACTTTCACTGCTTTTACCC
EGF	CTGGAAGCCTTTATAGAGCAG	CTTATCAAGCACATCCAATGA
GAPDH	CATGAGAAGTATGACAACAGCCT	AGTCCTTCCACGATACCAAAGT

Table S3. IC50 values of anlotinib in ATC cell lines. IC50 50% inhibitory concentration.

ATC cell lines	IC 50 (μM)					
	24 h		48 h		72 h	
	Normoxia	Hypoxia	Normoxia	Hypoxia	Normoxia	Hypoxia
KHM-5M	7.22	6.95	4.11	3.88	3.25	3.06
CAL-62	8.62	8.24	4.96	4.80	4.05	3.88
C643	12.57	12.14	7.35	7.15	5.22	5.07
BHT-101	5.58	5.40	3.21	3.12	2.95	2.90
BCPAP	16.15	15.87	9.12	8.75	6.45	6.39
Nthy-ori 3-1	42.85	41.60	19.25	19.10	17.22	17.05

Fig S1

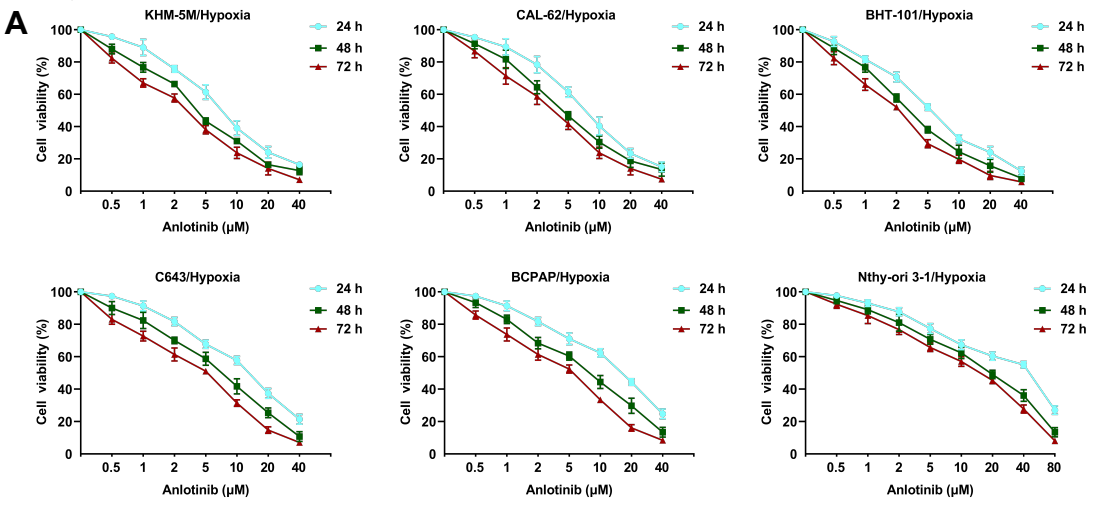
A
KHM-5M/Hypoxia
CAL-62/Hypoxia
BHT-101/Hypoxia
C643/Hypoxia
BCPAP/Hypoxia
Nthy-ori 3-1/Hypoxia
24 h
48 h
72 h
Cell viability (%)
Anlotinib (μM)

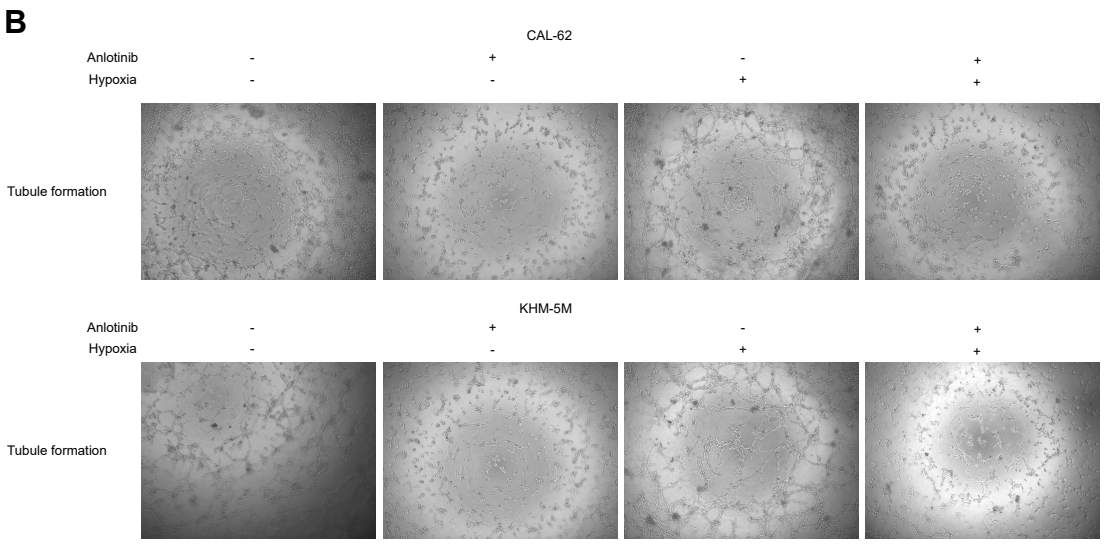
B
CAL-62
KHM-5M
Anlotinib
Hypoxia
Tubule formation

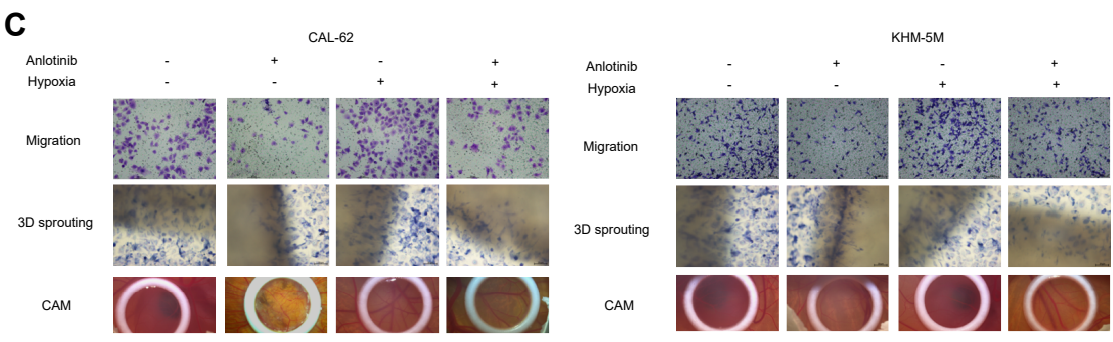
C
CAL-62
KHM-5M
Anlotinib
Hypoxia
Migration
3D sprouting
CAM

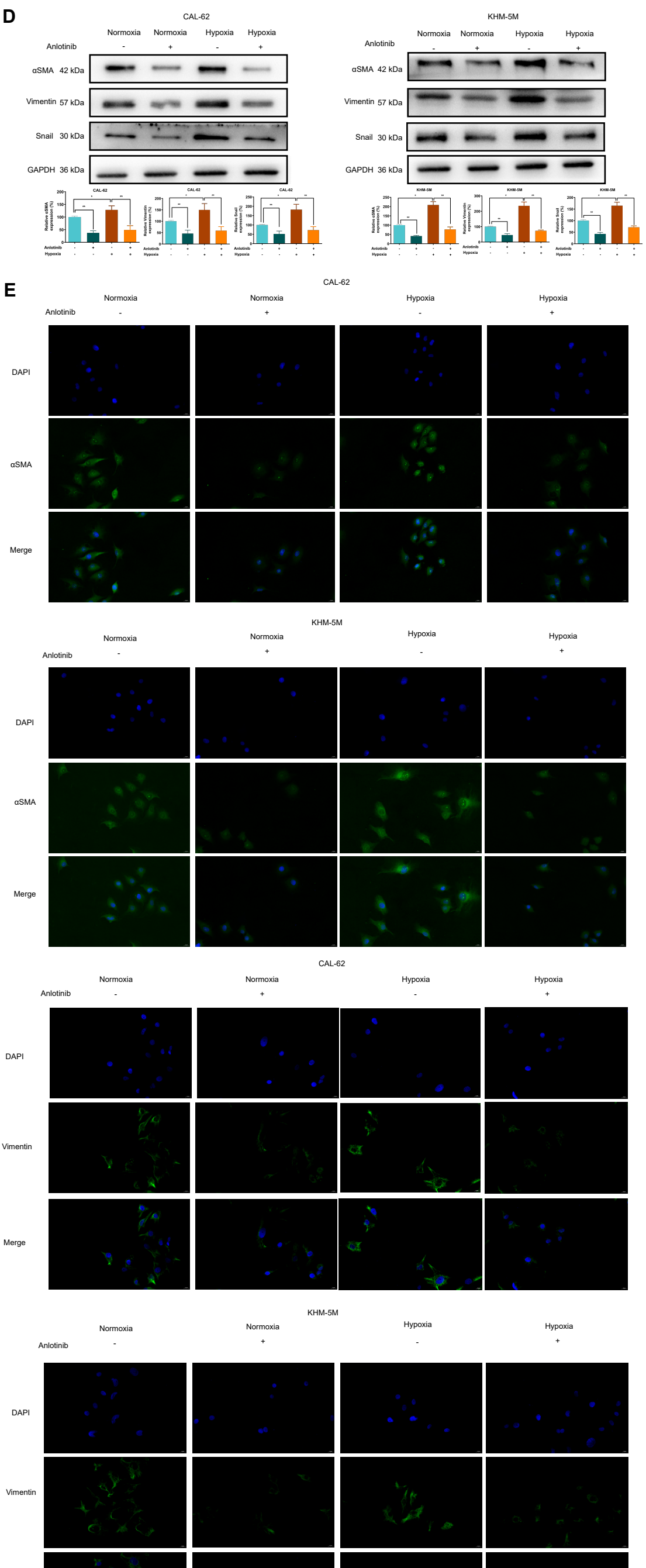
D
CAL-62
KHM-5M
Normoxia
Hypoxia
Anlotinib
αSMA 42 kDa
Vimentin 57 kDa
Snail 30 kDa
GAPDH 36 kDa
Relative αSMA expression (%)
Relative Vimentin expression (%)
Relative Snail expression (%)

E
CAL-62
KHM-5M
Normoxia
Hypoxia
Anlotinib
DAPI
αSMA
Merge
Vimentin
Relative gray value of αSMA (%)
Relative gray value of Vimentin (%)

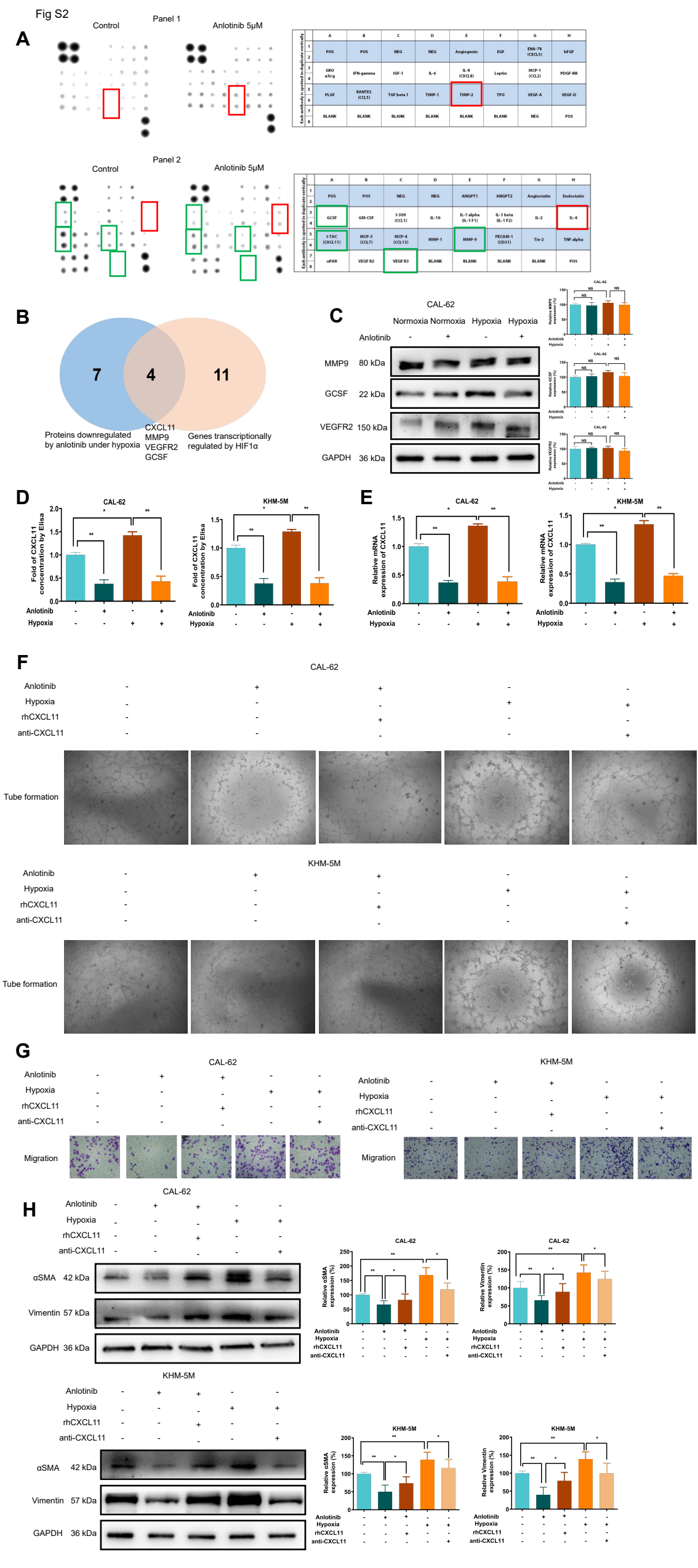
Fig S2
A
Control
Panel 1
Anlotinib 5μM
Each antibody is spotted in duplicate vertically
A B C D E F G H
1 2 POS POS NEG NEG Angiogenin EGF ENA-78 (CXCL5) bFGF
3 4 GRO a/b/g IFN-gamma IGF-1 IL-6 IL-8 (CXCL8) Leptin MCP-1 (CCL2) PDGF-BB
5 6 PLGF RANTES (CCL5) TGF beta 1 TIMP-1 TIMP-2 TPO VEGF-A VEGF-D
7 8 BLANK BLANK BLANK BLANK BLANK BLANK NEG POS
Panel 2
Control
Anlotinib 5μM
Each antibody is spotted in duplicate vertically
A B C D E F G H
1 2 POS POS NEG NEG ANGPT1 ANGPT2 Angiostatin Endostatin
3 4 GCSF GM-CSF I-309 (CCL1) IL-10 IL-1 alpha (IL-1 F1) IL-1 beta (IL-1 F2) IL-2 IL-4
5 6 I-TAC (CXCL11) MCP-3 (CCL7) MCP-4 (CCL13) MMP-1 MMP-9 PECAM-1 (CD31) Tie-2 TNF alpha
7 8 uPAR VEGF R2 VEGF R3 BLANK BLANK BLANK BLANK POS
B
7
4
11
Proteins downregulated by anlotinib under hypoxia
CXCL11
MMP9
VEGFR2
GCSF
Genes transcriptionally regulated by HIF1α
C
CAL-62
Normoxia Normoxia Hypoxia Hypoxia
Anlotinib - + - +
MMP9 80 kDa
GCSF 22 kDa
VEGFR2 150 kDa
GAPDH 36 kDa
Relative MMP9 expression (%)
Relative GCSF expression (%)
Relative VEGFR2 expression (%)
NS
D
CAL-62
KHM-5M
Fold of CXCL11 concentration by Elisa
Anlotinib - + - +
Hypoxia - - + +
E
CAL-62
KHM-5M
Relative mRNA expression of CXCL11
Anlotinib - + - +
Hypoxia - - + +
F
CAL-62
Anlotinib - + + - -
Hypoxia - - - + +
rhCXCL11 - - + - -
anti-CXCL11 - - - - +
Tube formation
KHM-5M
Anlotinib - + + - -
Hypoxia - - - + +
rhCXCL11 - - + - -
anti-CXCL11 - - - - +
Tube formation
G
CAL-62
Anlotinib - + + - -
Hypoxia - - - + +
rhCXCL11 - - + - -
anti-CXCL11 - - - - +
Migration
KHM-5M
Anlotinib - + + - -
Hypoxia - - - + +
rhCXCL11 - - + - -
anti-CXCL11 - - - - +
Migration
H
CAL-62
Anlotinib - + + - -
Hypoxia - - - + +
rhCXCL11 - - + - -
anti-CXCL11 - - - - +
αSMA 42 kDa
Vimentin 57 kDa
GAPDH 36 kDa
Relative αSMA expression (%)
Relative Vimentin expression (%)
KHM-5M
Anlotinib - + + - -
Hypoxia - - - + +
rhCXCL11 - - + - -
anti-CXCL11 - - - - +
αSMA 42 kDa
Vimentin 57 kDa
GAPDH 36 kDa
Relative αSMA expression (%)
Relative Vimentin expression (%)

Fig S3

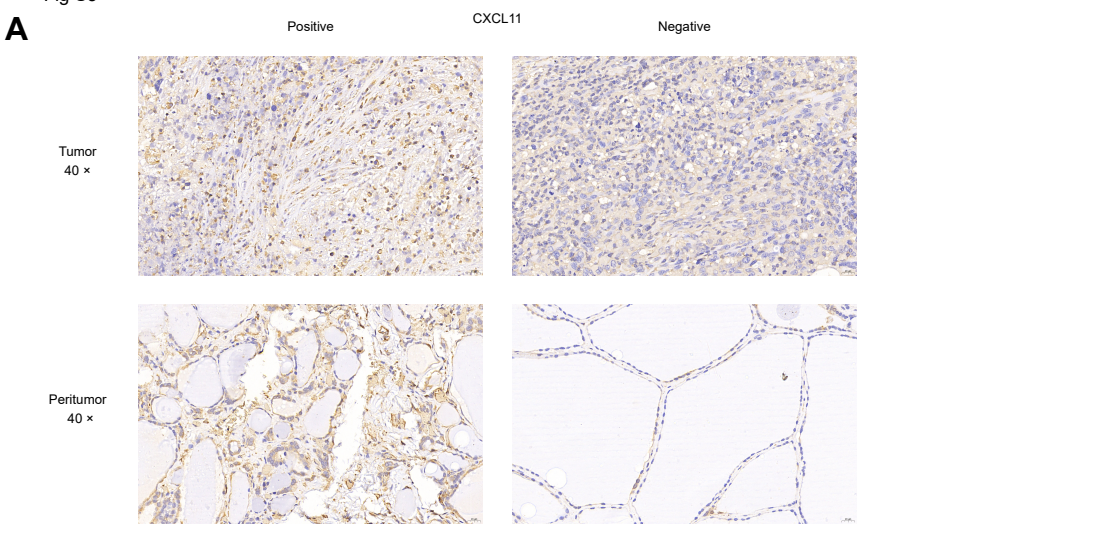
A
CXCL11
Positive
Negative
Tumor
40 ×
Peritumor
40 ×
B
BHT101 C643 KHM-5M CAL-62 BCPAP Nthy-ori 3-1
CXCL11 14 kDa
GAPDH 36 kDa
Relative CXCL11 expression (%)
BHT101 C643 KHM-5M CAL-62 BCPAP Nthy-ori 3-1
C
rhCXCL11
Time 0 2 h
Concentration 0 100 ng/mL
Tube formation
Migration
D
CAL-62
siNC siCXCL11
CXCL11 14 kDa
GAPDH 36 kDa
Relative CXCL11 expression (%)
Vector CXCL11
KHM-5M
E
rhCXCL11
CAL-62/ siNC -
CAL-62/ siCXCL11 -
CAL-62/ siCXCL11 +
KHM-5M/ siNC -
KHM-5M/ siCXCL11 -
KHM-5M/ siCXCL11 +
Tube formation
Migration
F
siNC siCXCL11 siCXCL11+ rhCXCL11
αSMA 42 kDa
Vimentin 57 kDa
GAPDH 36 kDa
Relative αSMA expression (%)
Relative Vimentin expression (%)
G
siNC
siCXCL11
siCXCL11+rhCXCL11
CCK-8 absorbance
Days
H
anti-CXCL11
CAL-62/ Vector -
CAL-62/ CXCL11 -
CAL-62/ CXCL11 +
KHM-5M/ Vector -
KHM-5M/ CXCL11 -
KHM-5M/ CXCL11 +
Tube formation
Migration
I
Vector CXCL11 CXCL11+ anti-CXCL11
αSMA 42 kDa
Vimentin 57 kDa
GAPDH 36 kDa
Relative αSMA expression (%)
Relative Vimentin expression (%)
J
Vector
CXCL11
CXCL11+anti-CXCL11
CCK-8 absorbance
Days
K
Relative mRNA expression of EGF
Relative mRNA expression of CXCL5
Relative mRNA expression of LEP
Relative mRNA expression of TPO
Relative mRNA expression of IFNG
Time
Concentration
rhCXCL11
HUVEC
L
siNC siCXCR7
CXCR7 42 kDa
GAPDH 36 kDa
Relative CXCR7 expression (%)
siNC siCXCR3
CXCR3 40 kDa
GAPDH 36 kDa
Relative CXCR3 expression (%)
M
Relative mRNA expression of EGF
siNC siNC siCXCR7 siCXCR3
rhCXCL11
N
Relative mRNA expression of CXCL11
siNC siNC siCXCR7 siCXCR3
rhCXCL11
O
HUVEC/ siNC +
HUVEC/ siCXCR7 +
rhCXCL11
PI
AnnexinV-FITC
1.40%
3.45%
94.87%
0.28%
1.86%
7.03%
90.24%
0.87%
Apoptotic cells (%)
HUVEC/ siNC
HUVEC/ siCXCR7
P
HUVEC
rhCXCL11
CXCR7 42 kDa
GAPDH 36 kDa
Relative CXCR7 expression (%)
Control
rhCXCL11
siNC siEGFR
Q
C643 BCPAP BHT101 CAL-62 KHM-5M HUVEC
CXCR7 42 kDa
GAPDH 36 kDa
Relative CXCR7 expression (%)
R
HUVEC/ siNC +
HUVEC/ siEGFR +
rhEGF
EGFR 150 kDa
p-EGFR (phospho Y1068) 130 kDa
αSMA 42 kDa
Vimentin 57 kDa
GAPDH 36 kDa
Relative EGFR expression (%)
Relative p-EGFR expression (%)
Relative αSMA expression (%)
Relative Vimentin expression (%)

Fig S4

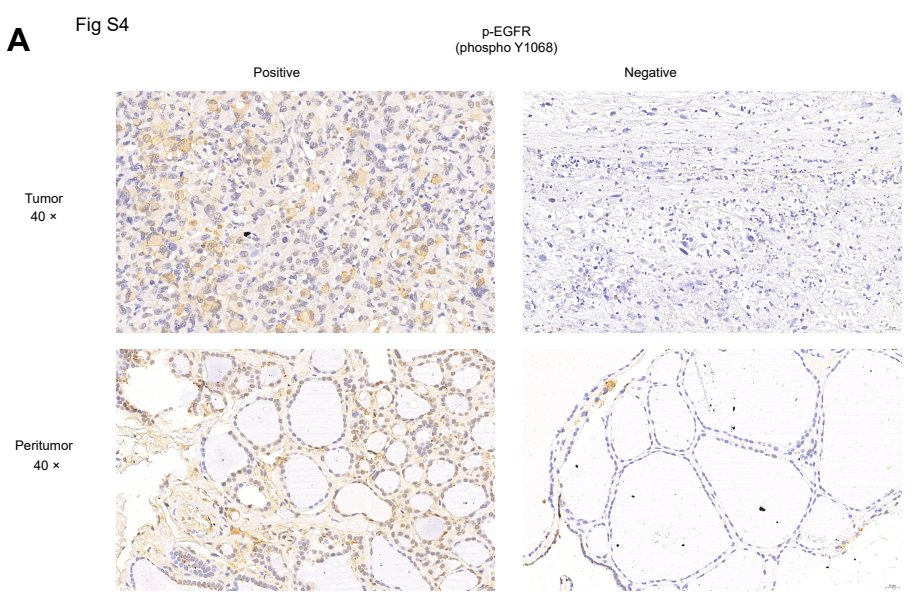
A
p-EGFR
(phospho Y1068)
Positive
Negative
Tumor
40 ×
Peritumor
40 ×

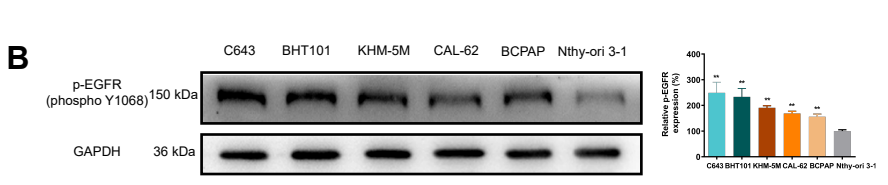
B
C643
BHT101
KHM-5M
CAL-62
BCPAP
Nthy-ori 3-1
p-EGFR
(phospho Y1068)
150 kDa
GAPDH
36 kDa
Relative p-EGFR expression (%)

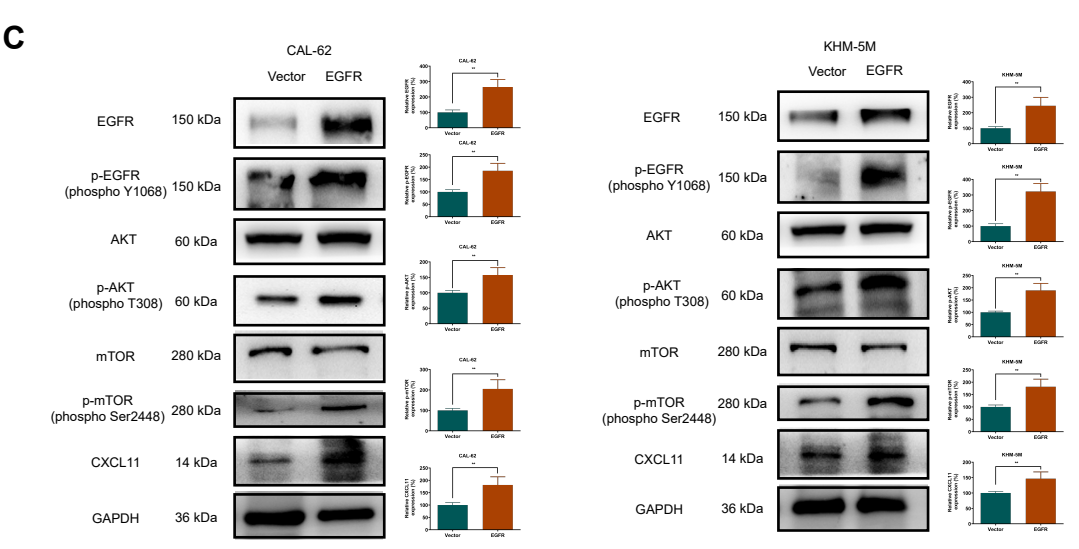
C
CAL-62
Vector
EGFR
KHM-5M
EGFR
150 kDa
p-EGFR
(phospho Y1068)
150 kDa
AKT
60 kDa
p-AKT
(phospho T308)
60 kDa
mTOR
280 kDa
p-mTOR
(phospho Ser2448)
280 kDa
CXCL11
14 kDa
GAPDH
36 kDa

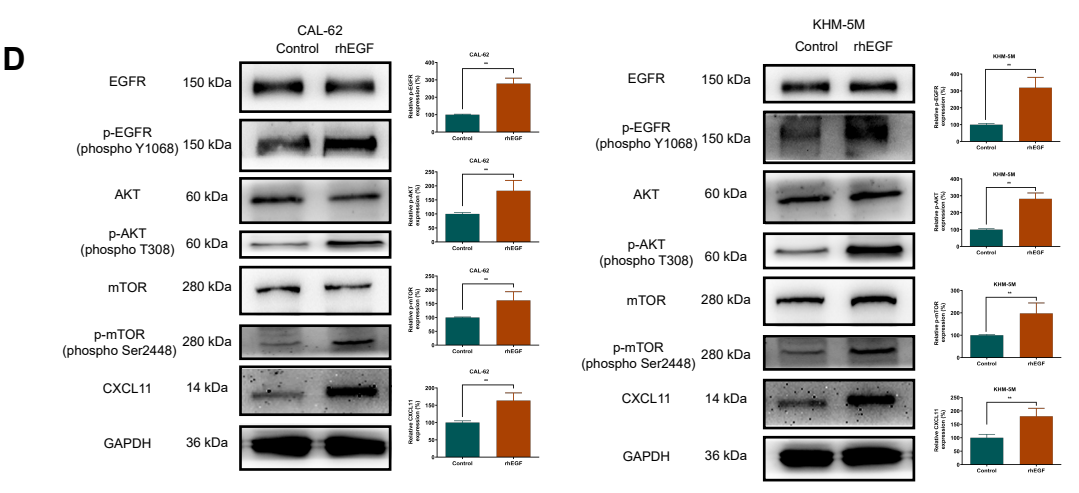
D
CAL-62
Control
rhEGF
KHM-5M
EGFR
150 kDa
p-EGFR
(phospho Y1068)
150 kDa
AKT
60 kDa
p-AKT
(phospho T308)
60 kDa
mTOR
280 kDa
p-mTOR
(phospho Ser2448)
280 kDa
CXCL11
14 kDa
GAPDH
36 kDa

E
CAL-62/
siNC
CAL-62/
siEGFR
CAL-62/
siEGFR
rhCXCL11
-
-
+
Tube formation
KHM-5M/
siNC
KHM-5M/
siEGFR
KHM-5M/
siEGFR
rhCXCL11
-
-
+
Tube formation
CAL-62/
siNC
CAL-62/
siEGFR
CAL-62/
siEGFR
rhCXCL11
-
-
+
Migration
KHM-5M/
siNC
KHM-5M/
siEGFR
KHM-5M/
siEGFR
rhCXCL11
-
-
+
Migration
F
CAL-62
siNC
siEGFR
siEGFR+
rhCXCL11
αSMA
42 kDa
Vimentin
57 kDa
GAPDH
36 kDa
KHM-5M
siNC
siEGFR
siEGFR+
rhCXCL11
αSMA
42 kDa
Vimentin
57 kDa
GAPDH
36 kDa
G
CAL-62/
Vector
CAL-62/
EGFR
CAL-62/
EGFR
anti-CXCL11
-
-
+
Tube formation
KHM-5M/
Vector
KHM-5M/
EGFR
KHM-5M/
EGFR
anti-CXCL11
-
-
+
Tube formation
CAL-62/
Vector
CAL-62/
EGFR
CAL-62/
EGFR
anti-CXCL11
-
-
+
Migration
KHM-5M/
Vector
KHM-5M/
EGFR
KHM-5M/
EGFR
anti-CXCL11
-
-
+
Migration
H
CAL-62
Vector
EGFR
EGFR+
anti-CXCL11
αSMA
42 kDa
Vimentin
57 kDa
GAPDH
36 kDa
KHM-5M
Vector
EGFR
EGFR+
anti-CXCL11
αSMA
42 kDa
Vimentin
57 kDa
GAPDH
36 kDa

Fig S5

A

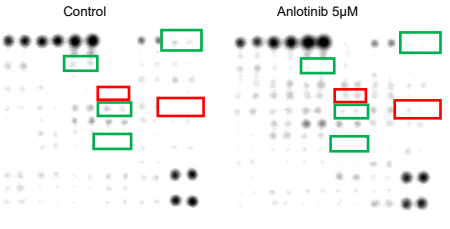

	A	B	C	D	E	F	G	H	I	J	K	L
1	POS1	POS1	POS2	POS2	POS3	POS3	ABL1	ABL1	ACK1	ACK1	ALK	ALK
2	NEG	NEG	NEG	NEG	Axl	Axl	Blk	Blk	BMX	BMX	Brk	Brk
3	Csk	Csk	Dtk	Dtk	EGFR	EGFR	EphA1	EphA1	EphA2	EphA2	EphA3	EphA3
4	EphA4	EphA4	EphA5	EphA5	EphA6	EphA6	EphA7	EphA7	EphA8	EphA8	EphB1	EphB1
5	EphB2	EphB2	EphB3	EphB3	EphB4	EphB4	EphB6	EphB6	ErbB2	ErbB2	ErbB3	ErbB3
6	ErbB4	ErbB4	FAK	FAK	FER	FER	FGFR1	FGFR1	FGFR2	FGFR2	FGFR2 (α isoform)	FGFR2 (α isoform)
7	Fgr	Fgr	FRK	FRK	Fyn	Fyn	Hck	Hck	HGFR	HGFR	IGF-IR	IGF-IR
8	Insulin R	Insulin R	Itk	Itk	JAK1	JAK1	JAK2	JAK2	JAK3	JAK3	LCK	LCK
9	LTK	LTK	Lyn	Lyn	MATK	MATK	M-CSFR	M-CSFR	MUSK	MUSK	NGFR	NGFR
10	PDGFR-α	PDGFR-α	PDGFR-β	PDGFR-β	PYK2	PYK2	RET	RET	ROR1	ROR1	ROR2	ROR2
11	ROS	ROS	RYK	RYK	SCFR	SCFR	SRMS	SRMS	SYK	SYK	Tec	Tec
12	Tie-1	Tie-1	Tie-2	Tie-2	TNK1	TNK1	TRKB	TRKB	TXK	TXK	NEG	NEG
13	Tyk2	Tyk2	TYRO10	TYRO10	VEGFR2	VEGFR2	VEGFR3	VEGFR3	ZAP70	ZAP70	POS4	POS4

B

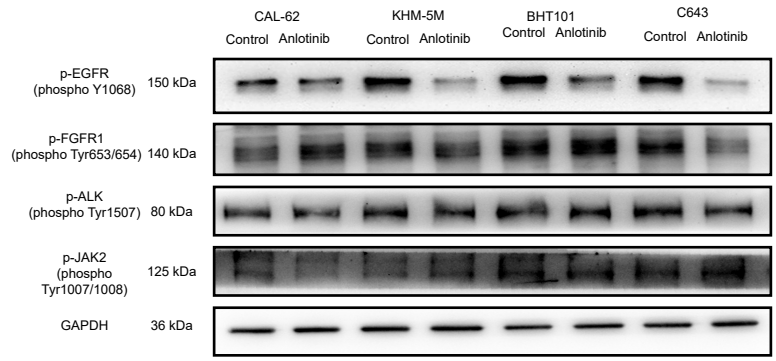

C

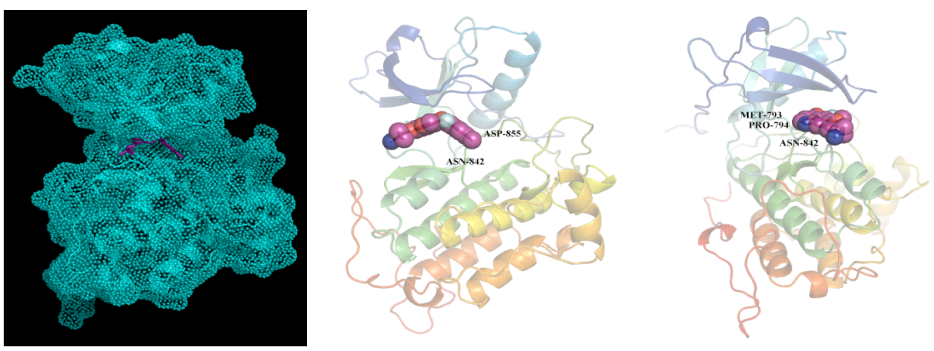

D